Structural Parameter of Orientational Order to Predict the Boson Vibrational Anomaly in Glasses

J. Yang,[1,2] Y. J. Wang,[1,2,*] E. Ma,[3] A. Zaccone,[4,5,6] L. H. Dai,[1,2] and M. Q. Jiang[1,2,†]

[1]*State Key Laboratory of Nonlinear Mechanics, Institute of Mechanics, Chinese Academy of Sciences, Beijing 100190, People's Republic of China*

[2]*School of Engineering Science, University of Chinese Academy of Sciences, Beijing 101408, People's Republic of China*

[3]*Department of Materials Science and Engineering, John Hopkins University, Baltimore, Maryland 21218, USA*

[4]*Department of Chemical Engineering and Biotechnology, University of Cambridge, Cambridge CB2 3RA , United Kingdom*

[5]*Cavendish Laboratory, University of Cambridge, Cambridge CB3 9HE, United Kingdom*

[6]*Department of Physics, University of Milan, via Celoria 16, 20133 Milan, Italy*

It has so far remained a major challenge to quantitatively predict the boson peak, a THz vibrational anomaly universal for glasses, from features in the amorphous structure. Using molecular dynamics simulations of a model $Cu_{50}Zr_{50}$ glass, we decompose the boson peak to contributions from atoms residing in different types of Voronoi polyhedra. We then introduce a microscopic structural parameter to depict the "orientational order", using the vector pointing from the center atom to the farthest vertex of its Voronoi

coordination polyhedron. This order parameter represents the most probable direction of transverse vibration at low frequencies. Its magnitude scales linearly with the boson peak intensity, and its spatial distribution accounts for the quasi-localized modes. This correlation is shown to be universal for different types of glasses.

Atomic vibrations in crystals are well understood as lattice waves, and their energy can be quantized as quasi-particles termed phonons. At low frequencies, the lattice waves can be treated as continuum elastic waves, and the vibrational density of states (VDOS) can be approximated using the Debye squared-frequency law, $g(\omega) \propto \omega^2$, with ω being the phonon frequency. For glasses lacking long-range order, however, their low-frequency VDOS universally displays an excess over the Debye level, forming the celebrated boson peak (BP). Such an anomaly implies that, around the BP frequency, disordered glasses can no longer be regarded as homogenous elastic medium; instead, they are spatially elastic-heterogeneous [1-4]. In particular, transverse phonons scatter strongly [3,4], producing additional localized modes [5,6]. It has been suggested that these quasi-localized low-frequency modes make up the BP [2,7,8]. An alternative view is that the BP does not involve additional modes but is just the counterpart of the transverse acoustic (TA) van Hove singularity in crystals, shifted to lower frequencies because of the structural disorder or low density of glasses [9-11]. The complex nature of the BP, ranging from extended TA waves to highly localized modes [3,12], constitutes one of the most fascinating problems in condensed matter physics.

Considerable efforts have been made to identify the dynamic or structural signatures of the BP. Grigera et al. [13] found that the BP can only survive in an inherent-structure (IS)-dominated glass with phonons, but disappears when the glass approaches a phonon-free, saddle-point-dominated phase. Furthermore, the phonons associated with the BP are of a transverse character [14,15]. A direct support is that the BP frequency coincides with the Ioffe-Regel limit of transverse phonons [2,6], at which the mean free path of transverse phonons becomes similar to their wavelength, causing significant scattering of the phonons. Consequently, their eigenvectors tend to localize in some defective or low-modulus regions where atoms vibrate with larger mean-square displacements (MSD) or amplitudes [4-6,16,17]. This leads to apparently localized modes resonantly coupled with the (weak) background transverse phonons. Such hybrid states are termed quasi-localized modes. The structural origin is believed to be related to the local regions that are more defective (usually having lower density or higher volume compared to the system average [2,5,18,19]). Recently, Ding et al. [20] found that these local "soft spots" are enriched in geometrically unfavored motifs (GUMs), participating preferentially in the quasi-localized low-frequency modes. Milkus and Zaccone [21] further argued that these GUMs actually represent the local breaking of center-inversion structural symmetry. In addition, Guerdane and Teichler [22] proposed a dynamical model of local order, and discovered that the BP is closely related to atoms whose coordination number (CN) fluctuations in a highly time-dependent manner. Despite of these advances, it remains a formidable challenge to quantitatively predict the BP properties directly from a structural parameter of the glass.

In this Letter, we accomplish this challenging task using molecular dynamics simulations of a prototypical model glass. A simple structural vector is identified as the tell-tale orientational order parameter underlying the vibrational modes corresponding to the BP, with predictive power of its intensity and frequency.

We start from a $Cu_{50}Zr_{50}$ model glass containing 221,184 atoms interacting with a Finnis-Sinclair type embedded-atom method (EAM) potential [23]. A small sample is first prepared by a heating-quenching technique, and then replicated by 3×3×3 to obtain the final sample with dimensions of ~15.66×15.66×15.66 nm^3 after a proper sub-T_g annealing [24,25] and subsequent cooling procedure to eliminate the artificial boundary effect. The glassy state of the obtained sample is carefully examined; see Fig. S1. Based on the IS of the glass, Voronoi tessellation is used to characterize the short-range order (SRO) of the vibrating atoms. The VDOS $g(\omega)$ of the glass is calculated by taking the Fourier transformation of the velocity auto-correlation function $\psi(t)$ [6,22,26,27]. The VDOS of those atoms surrounded by a specific type of Voronoi polyhedron can be directly calculated by extracting $\psi(t)$ of the selected atoms. The BP can be determined by plotting the reduced VDOS $g(\omega)/\omega^2$ over ω. As a reference, the Debye level $g_D(\omega)/\omega^2$ is estimated to be ~87.23 μTHz^{-3} for the present glass. More details of the calculations are provided in the Supplementary Material [28].

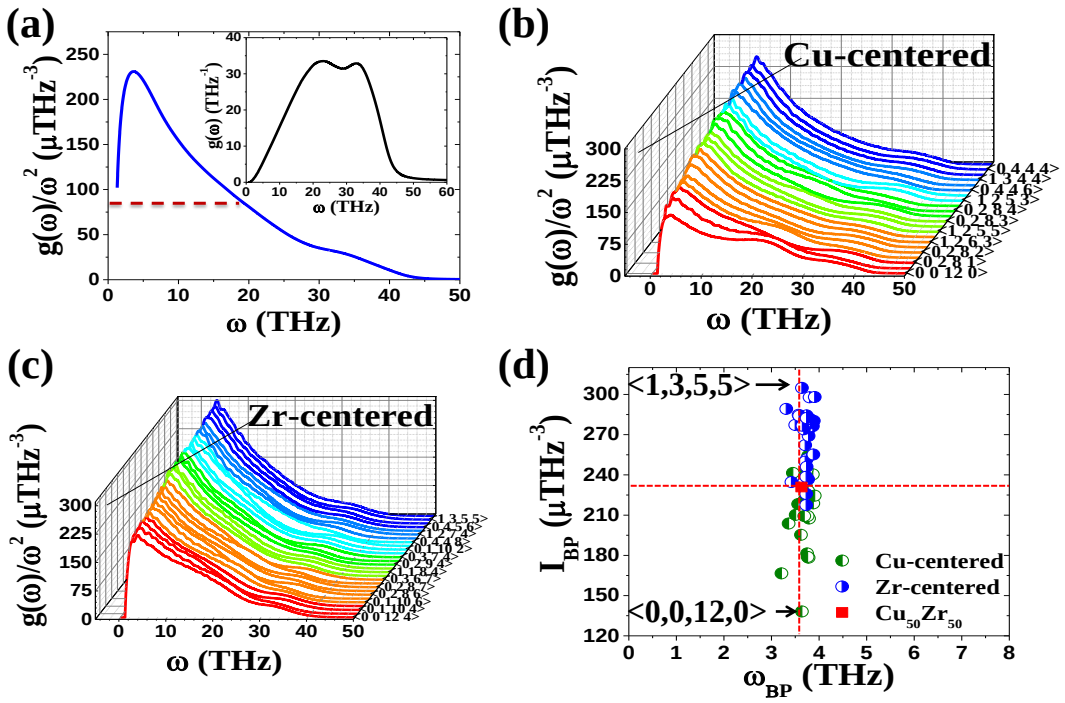

FIG. 1. (a) Reduced VDOS $g(\omega)/\omega^2$ of the $Cu_{50}Zr_{50}$ glass. The dashed line shows the Debye level. Inset: VDOS $g(\omega)$. Reduced VDOSs $g(\omega)/\omega^2$ of (b) the Cu atoms and (c) the Zr atoms surrounded by different types of Voronoi polyhedra. For readability of the legends in the limited space available in both (b) and (c), the Voronoi indices are marked only for selected polyhedra. (d) Intensities I_{BP} of BPs versus their characteristic frequencies ω_{BP} for all types of atoms and the entire glass. The horizontal and vertical dashed lines benchmark the position of ensemble averaged value for the entire glass.

Figure 1(a) displays the reduced VDOS, $g(\omega)/\omega^2$, of the $Cu_{50}Zr_{50}$ glass, and the corresponding VDOS $g(\omega)$ in the inset. A BP (maximum at ~3.63 THz) can be clearly observed over the Debye level. We next sorted out the contributions of atoms within different SROs (i.e., in various local structures) to the observed BP. The SROs of atoms are characterized using their Voronoi polyhedra (the most frequent 50 include

22 Cu-centered and 28 Zr-centered polyhedra [28]). The present equimolar binary glass consists of a spectrum of SROs, with no one predominating; see Fig. S2. The reduced VDOS $g(\omega)/\omega^2$ for these polyhedra of the Cu and Zr atoms are plotted in Figs. 1(b) and 1(c), respectively. As expected, atoms of different SROs display different degrees of BPs. These BPs are arranged from the weakest to the strongest (from front to back). For Cu atoms in Cu-centered Voronoi polyhedra, their BPs increase in the sequence of <0,0,12,0>, <1,0,9,3>, <0,2,8,1>, …, <1,3,5,2>, <0,4,4,4>, and <0,4,4,5>. For Zr-centered polyhedra, the sequence becomes <0,0,12,3>, <0,0,12,4>, <0,0,12,2>, …, <0,4,5,6>, <1,2,7,3>, and <1,3,5,5>. In general, compact and more symmetrical polyhedra are less conducive to low-frequency vibrations, thus incurring relatively weak BPs. In contrast, the GUMs make strong and disproportional contributions to the low-frequency BPs, similar to the case in $Cu_{64}Zr_{36}$ glass [20]. Figure 1(d) summarizes the characteristic intensities I_{BP} and frequencies ω_{BP} of the BPs corresponding to all types of polyhedra. It is found that I_{BP} varies remarkably from the smallest 138.16 μTHz^{-3} of Cu-centered <0,0,12,0> to the largest 298.07 μTHz^{-3} of Zr-centered <1,3,5,5>. However, all ω_{BP} data reside in a rather narrow range of 3-4 THz around the BP frequency (~3.63 THz) of the entire sample. This provides solid evidence for the phonon feature of the BPs. That is to say, all atoms, no matter in what local structural environments, participate in the low-frequency vibrations around the BP. These partial BP vibrations within different SROs are strongly coupled, and their characteristic frequency is determined by the overall spatial distribution of these SROs, rather than their individual local structures. If these partial vibrations are absolutely isolated, their

intensities and frequencies should follow an inversely linear relationship, as observed in different glass systems [29]. Instead, they contribute differently to the full BP, as evidenced by the spread of their I_{BP}, deviating from the BP intensity (~230.97 μTHz^{-3}) of the entire sample. We also note that the Zr-centered polyhedra generally have higher BPs compared to the Cu-centered ones.

The challenge then is to find a structural parameter that quantitatively scales with the BP intensity, beyond the vague topological descriptor above (Voronoi indices). Obviously, it is not the CN of nearest-neighbor atoms. The volume, and the fraction of five-fold faces, of the Voronoi polyhedra also show no clear correlation with the BP intensity; see Figs. S7 and S8, respectively. For example, we notice that the distorted Cu-centered <1,0,9,3> atoms do not show the strong BP.

We next look into the dynamics underlying the BP to ferret out the controlling structural feature. We first calculated the vibrational MSD of the center atom in the 22 Cu-centered and 28 Zr-centered polyhedra [28]. It is found that the MSD is linearly correlated with their BP intensities, but the two lines for Cu and Zr atoms are separated; see Fig. S9(a). After scaling the MSD with the Voronoi volume, the resultant "flexibility volume" [16] also shows a similar correlation with the BP intensity; see Fig. S9(b). But again the correlation with Cu is separated from that for Zr. These correlations are composition dependent and species-specific, indicating that the vibrational MSD alone is insufficient to predict the BP intensity for all types of atoms. For example, the Zr-centered <1,3,5,5> atoms with the highest BP do not have the largest MSD. And, the Cu-centered <0,4,4,5> atoms have the largest MSD, but do not exhibit the strongest BP.

On average, compared with the Cu atoms, the Zr atoms have lower MSD, but their BP intensities are higher; see Figs. S9(a) and 1(d). Such a paradox means that the excess low-frequency modes at the BP depend on not only the atomic vibrational MSD, but also the vibrating atomic species themselves.

We note that the atomic vibrations are directional, with clear local anisotropy dependent on the SROs or Voronoi configurations. This information is hidden in the overall atomic MSD [30], and needs to be separated out to quantitatively predict the BP. To this end, we define a new quantity, termed directionally vibrational MSD for each atom i, $\left\langle r_i^2 \right\rangle^\alpha = \left\langle \left(\Delta\vec{r}_i(t) \cdot \vec{d}_i^{\,\alpha} \Big/ \left|\vec{d}_i^{\,\alpha}\right| \right)^2 \right\rangle$, where $\Delta\vec{r}_i(t)$ is the atomic vibrational displacement that measures the deviation of the instantaneous position from its equilibrium position in the IS, $\vec{d}_i^{\,\alpha}$ are a series of vectors pointing from the center of the atom *i* to the vertex α of its Voronoi polyhedron [Fig. 2(a)], $\left|\vec{d}_i^{\,\alpha}\right|$ is the length of $\vec{d}_i^{\,\alpha}$, and the angular brackets denote the average over time. The $\left\langle r_i^2 \right\rangle^\alpha$ *per se* is the projection of the atomic vibrational MSD in the direction of vector $\vec{d}_i^{\,\alpha}$. Physically, a large $\left\langle r_i^2 \right\rangle^\alpha$ means the atom *i* prefers a low-frequency vibration in the direction towards the α vertex. It is noteworthy that the directional vibrations capture the transverse character, because the vectors $\vec{d}_i^{\,\alpha}$ always point at the possible shear directions. Figure 2(b) plots the sample-averaged $\left\langle r^2 \right\rangle^\alpha$ versus $\left\langle \left|\vec{d}_i^{\,\alpha}\right| \right\rangle$; here only the 20 longest $\vec{d}_i^{\,\alpha}$ for each atom are considered. It is interesting to find that $\left\langle r^2 \right\rangle^\alpha$ and $\left\langle \left|\vec{d}_i^{\,\alpha}\right| \right\rangle$ are linearly correlated. The longer the $\left\langle \left|\vec{d}_i^{\,\alpha}\right| \right\rangle$ is, the larger the $\left\langle r^2 \right\rangle^\alpha$ (corresponding to the modes of lower frequencies). Therefore, Fig. 2(b) clearly

demonstrates that the low-frequency vibrations of the entire system prefer the vector field $\vec{d}_i^{\,\alpha}$, each pointing from the center atom to the farthest vertex of its coordination polyhedron. This behavior is confirmed for each and every constituent species. For each species residing in the same type of Voronoi polyhedron, the atomic $\langle r^2 \rangle^{\alpha}$ still follows a linear relationship with $\langle |\vec{d}_i^{\,\alpha}| \rangle$; see Fig. S10.

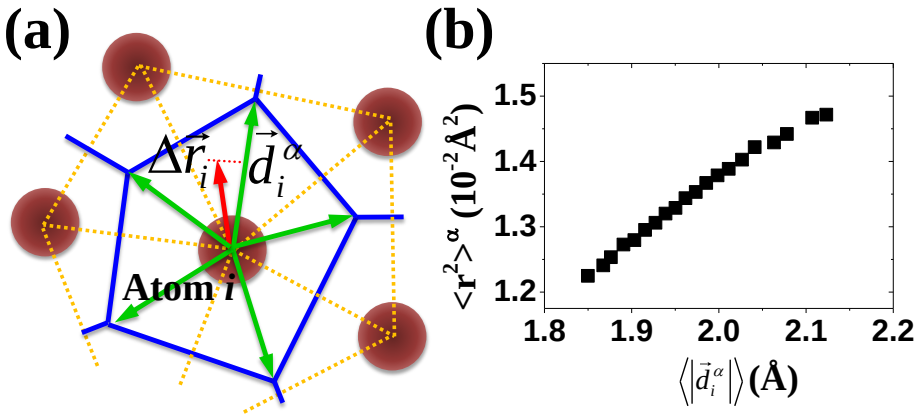

FIG. 2. (a) A schematic of an atom's Voronoi polyhedron (blue lines). Red arrow: the atomic vibrational displacement $\Delta\vec{r}_i(t)$. Green arrows: vectors $\vec{d}_i^{\,\alpha}$ pointing from each atom center to the vertices of its Voronoi polyhedron. (b) Projections of $\Delta\vec{r}_i(t)$ onto $\vec{d}_i^{\,\alpha}$ for different $|\vec{d}_i^{\,\alpha}|$ averaged for all atoms in the glass.

We shall define the vectors $\vec{d}_i^{\,\alpha}$ having the largest length as the orientational order $\vec{\Theta}_i^{\mathrm{BP}}$ of the BP, and its length $|\vec{\Theta}_i^{\mathrm{BP}}| = \max|\vec{d}_i^{\,\alpha}|$. This structural parameter $\vec{\Theta}_i^{\mathrm{BP}}$ identifies the most probable direction of transverse vibrations, the one with the largest vibrational MSD $\langle r^2 \rangle_i^{\alpha}$ and hence the lowest frequency, and its length $|\vec{\Theta}_i^{\mathrm{BP}}|$ represents the highest degree of symmetry-breaking for the environments in which the atoms vibrate. In the $\vec{\Theta}_i^{\mathrm{BP}}$ direction, the atom can move or be displaced with little energy. This is opposite to other directions where there is less space to move, the atom

is constrained and displacements cost more energy. Therefore, $\vec{\Theta}_i^{\mathrm{BP}}$ should be a useful measure of the BP. To confirm this, we plot the BP intensity I_{BP} against $\left\langle \left| \vec{\Theta}_i^{\mathrm{BP}} \right| \right\rangle$ averaged over each atomic species and over the entire sample, as shown in Fig. 3. The correlation between I_{BP} and $\left\langle \left| \vec{\Theta}_i^{\mathrm{BP}} \right| \right\rangle$ is obvious, and can be satisfactorily fitted using a linear relationship with the Pearson correlation coefficient of ~0.92. Unlike the vibrational MSD or flexibility volume, the data of all I_{BP} and the structural parameter $\left| \vec{\Theta}_i^{\mathrm{BP}} \right|$ collapse onto a general straight line, regardless of which atomic species and including the average over the entire sample. This implies that the $\left| \vec{\Theta}_i^{\mathrm{BP}} \right|$ has incorporated the information from both the vibrational MSD and the species (Cu or Zr) involved; here the atomic species are distinguished by their sizes, since $\left| \vec{\Theta}_i^{\mathrm{BP}} \right|$ is a length parameter. Moreover, the vibrational property I_{BP} is very sensitive to $\left| \vec{\Theta}_i^{\mathrm{BP}} \right|$: an increase of the latter by about 7% more than doubles the former. To the best of our knowledge, this is the first time one can quantitatively correlate the BP intensity with a simple structural parameter.

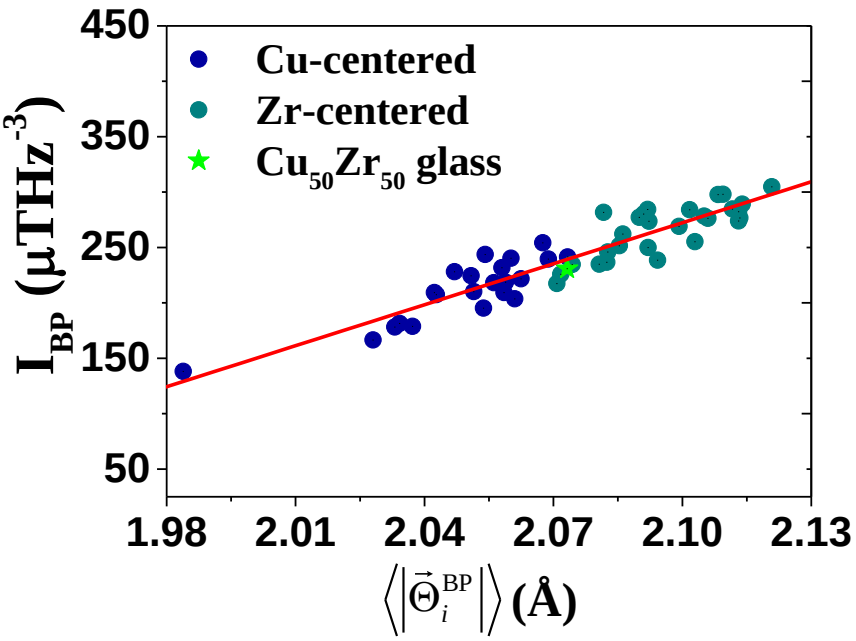

FIG. 3. Correlation between the BP intensity I_{BP} and the length parameter $\langle|\vec{\Theta}_i^{BP}|\rangle$, averaged over all the atoms of each species, and over all atoms in the glass. The red straight line is a linear fit to the data.

Next, we demonstrate the quasi-localized feature of BP from the new orientational order $\vec{\Theta}_i^{BP}$. We plot the spatial distribution of $\vec{\Theta}_i^{BP}$ (black arrows) for individual atoms (red filled circles). Fig. 4(a) through (c) each shows a representative cross-sectional view (4 Å in thickness), along one of the three different directions. The length of the black arrows represents the $|\vec{\Theta}_i^{BP}|$ of each atom. The size of the filled circles denotes the BP intensity I_{BP} associated with this atom. Here, the data of either $\vec{\Theta}_i^{BP}$ or I_{BP} are averaged over atoms that reside in polyhedra having the same Voronoi indices. Figure 4, from the spatial perspective, further confirms that atoms with larger orientation order $\vec{\Theta}_i^{BP}$ contribute more to the I_{BP} of the BP: longer black arrows correspond to larger red circles [Fig. 4(d)]. Also, the high-$|\vec{\Theta}_i^{BP}|$ atoms have a tendency

to aggregate into local patches as fertile “soft spots” for low-frequency transverse vibrations. This picture looks very similar to the spatial distribution of the vibrational amplitude around the BP frequency reported by Shintani and Tanaka [2], and is also reminiscent of the contour plot of the participation fraction of low-frequency normal modes reported by Widmer-Cooper et al. [31]. These findings clearly confirm the quasi-localized nature of the BP vibrations. In this scenario, the BP frequency ω_{BP} of the glass is equal to the Ioffe-Regel limit of transverse phonons. Thus the limit wavelength $\lambda_{\mathrm{phon}}^{\mathrm{IR}}$ of phonons is estimated as $\lambda_{\mathrm{phon}}^{\mathrm{IR}} \approx 2\pi c_T / \omega_{\mathrm{BP}}$, where c_T is the transverse phonon velocity. The calculated $\lambda_{\mathrm{phon}}^{\mathrm{IR}}$ of about 2.6 nm is close to the characteristic length of the heterogeneous $\vec{\Theta}_i^{\mathrm{BP}}$ [see magnified view in Fig. 4(d)]. A slight difference may arise from two possible reasons. One is that we do not distinguish atoms residing in the Voronoi polyhedra with identical indices. The other is that it is very difficult to precisely calculate c_T, which is strongly frequency dependent and has pronounced spatial fluctuation at this limit. Nevertheless, we believe that the entire spatial distribution of the locally varying $\vec{\Theta}_i^{\mathrm{BP}}$ acts as a global feature that determines the characteristic frequency ω_{BP} of the glass. This is consistent with Fig. 1(d).

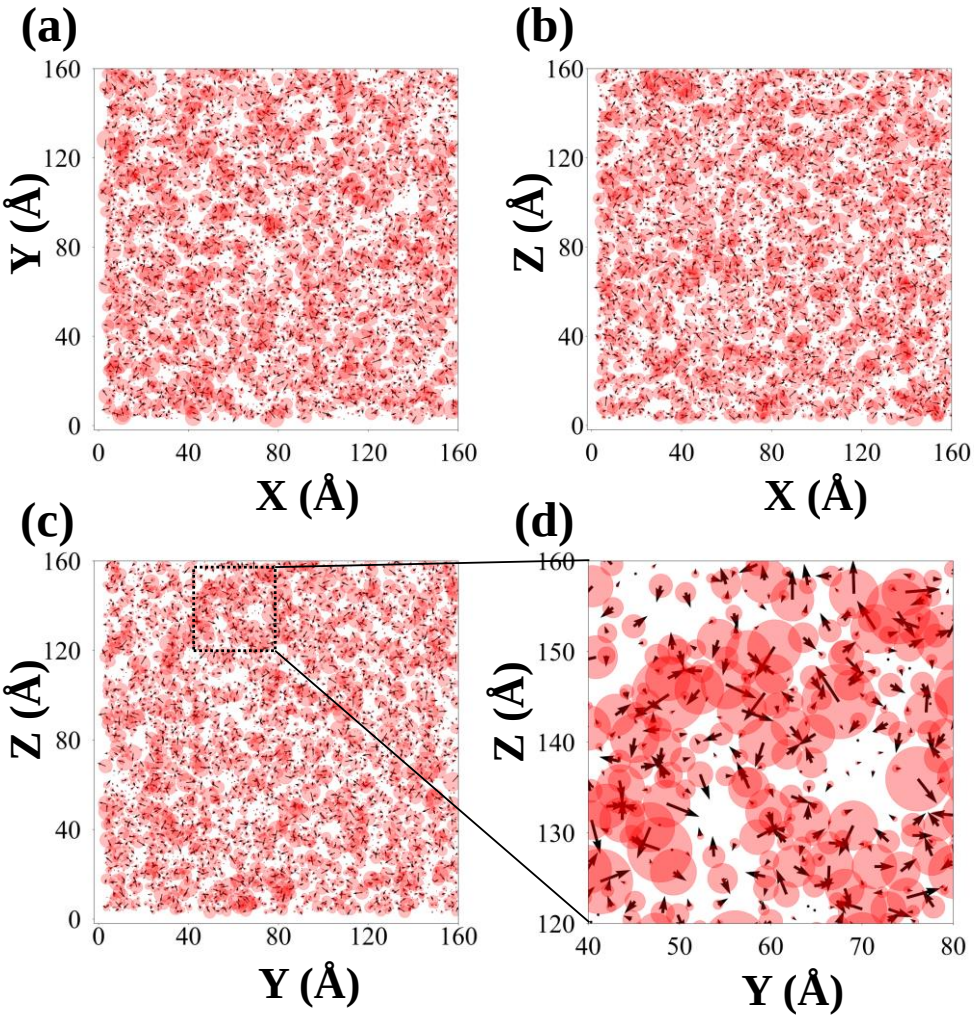

FIG. 4. Representative (a) X-Y, (b) X-Z and (c) Y-Z cross-sections show the spatial distribution of the orientational order $\vec{\Theta}_i^{\mathrm{BP}}$ (black arrows) for individual atoms (red filled circles). The length of arrows represents $\left|\vec{\Theta}_i^{\mathrm{BP}}\right|$. The size of circles denotes the BP intensity I_{BP}. (d) is a partial magnification of (c).

Finally, we demonstrate the universality of the orientational order of BPs by examining another 11 glasses, including Ta, Zr, $Co_{80}Al_{20}$, $Ni_{80}P_{20}$, $Ni_{80}Zr_{20}$, $Pd_{80}Si_{20}$, $Al_{80}Cu_{20}$, $Cu_{64}Zr_{36}$, $Cu_{50}Zr_{50}$, $Cu_{46}Zr_{46}Al_8$, as well as the general Lennard-Jones (L-J) model. These glasses are of different types, covering monatomic, binary, and ternary systems of different bonding characteristics. Details about the computer simulations are

given in Supplemental Material [28]. The BP intensity I_{BP} and the sample-averaged $\left\langle \left| \vec{\Theta}_i^{\mathrm{BP}} \right| \right\rangle$ for all the 12 glasses are plotted in Fig. 5. It is striking to find that a general linear correlation still holds, indicating the robustness of the orientational order in predicting BP across a wide range of glass compositions. It is therefore believed that the anisotropic vibrations with orientational order are a general physical origin of the mysterious BP in glasses. Further evidence comes from the clear correlation between the orientational order and the time-dependent CN fluctuations; see Fig. S14. It has been demonstrated that atoms with higher CN-fluctuations or frequent cage-breaking contribute more to the BP [22].

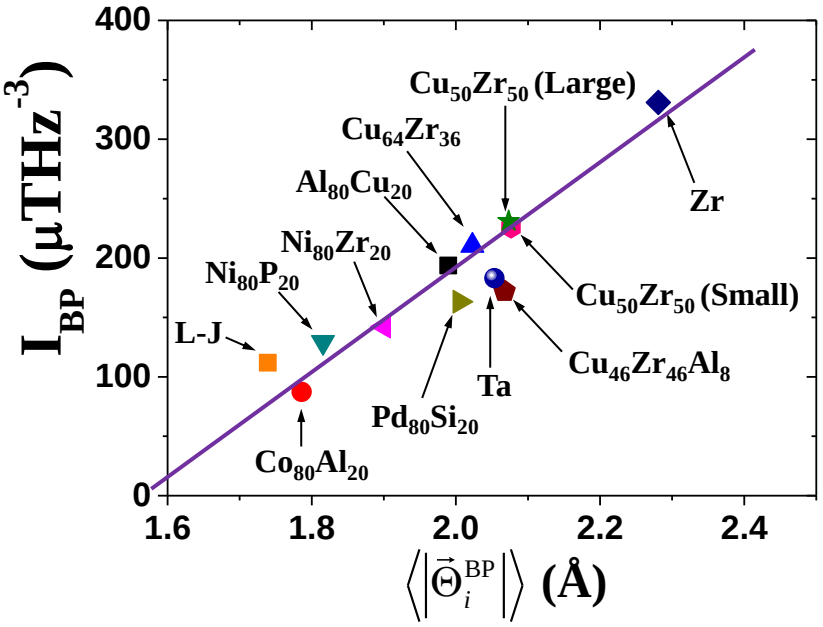

FIG. 5. Correlation between I_{BP} and $\left\langle \left| \vec{\Theta}_i^{\mathrm{BP}} \right| \right\rangle$ for a wide range of glasses. The solid line serves as a guide for the eye.

To summarize, the VDOS and BP anomaly of a prototypical model $Cu_{50}Zr_{50}$

metallic glass are investigated using MD simulations. It is revealed that all atoms participate in the vibrational modes around the BP frequency, but the BP contribution of each type of atoms strongly depends on the local SRO environments in which they vibrate. We further identify a series of structural vectors, termed orientational order, pointing from the center of each atom to the farthest vertex of its coordination polyhedron, as the most probable direction of transverse vibrations at low frequencies. It is found that the magnitude (length) of the orientational order parameter determines the BP intensity, and its spatial distribution produces the quasi-localized modes of BP. Last but not least, these findings appear to be universally applicable to a wide range of glasses.

This work was supported by the NSFC (Grant Nos. 11522221, 11790292 and 11672299), the Strategic Priority Research Program (Grant No. XDB22040303), and the Key Research Program of Frontier Sciences (Grant No. QYZDJSSW-JSC011) of CAS. E.M. is supported at JHU by US-NSF-DMR 1505621.

*yjwang@imech.ac.cn

†mqjiang@imech.ac.cn

[1] W. Schirmacher, G. Ruocco, and T. Scopigno, Phys. Rev. Lett. **98**, 025501 (2007).

[2] H. Shintani and H. Tanaka, Nat. Mater. **7**, 870 (2008).

[3] S. Gelin, H. Tanaka, and A. Lemaitre, Nat. Mater. **15**, 1177 (2016).

[4] L. Zhang, J. Zheng, Y. Wang, L. Zhang, Z. Jin, L. Hong, Y. Wang, and J. Zhang, Nature Commu. **8**, 67 (2017).

[5] B. B. Laird and H. R. Schober, Phys. Rev. Lett. **66**, 636 (1991).

[6] N. Jakse, A. Nassour, and A. Pasturel, Phys. Rev. B **85**, 174201 (2012).

[7] H. R. Schober, J. Non-Cryst. Solids **357**, 501 (2011).

[8] P. M. Derlet, R. Maaß, and J. F. Löffler, Eur. Phys. J. B **85**, 148 (2012).

[9] A. I. Chumakov *et al.*, Phys. Rev. Lett. **106**, 225501 (2011).

[10] A. I. Chumakov *et al.*, Phys. Rev. Lett. **112**, 025502 (2014).

[11] P. Benassi, A. Fontana, W. Frizzera, M. Montagna, V. Mazzacurati, and G. Signorelli, Philos.

Mag. B **71**, 761 (1995).
[12] R. Zorn, Physics **4**, 44 (2011).
[13] T. S. Grigera, V. Martin-Mayor, G. Parisi, and P. Verrocchio, Nature **422**, 289 (2003).
[14] R. J. Nemanich, Phys. Rev. B **16**, 1655 (1977).
[15] D. Caprion, P. Jund, and R. Jullien, Phys. Rev. Lett. **77**, 675 (1996).
[16] J. Ding, Y.-Q. Cheng, H. Sheng, M. Asta, R. O. Ritchie, and E. Ma, Nature Commu. **7**, 13733 (2016).
[17] H. Shen, P. Tan, and L. Xu, Phys. Rev. Lett. **116**, 048302 (2016).
[18] R. Biswas, A. M. Bouchard, W. A. Kamitakahara, G. S. Grest, and C. M. Soukoulis, Phys. Rev. Lett. **60**, 2280 (1988).
[19] B. Huang, H. Y. Bai, and W. H. Wang, J. Appl. Phys. **115**, 153505 (2014).
[20] J. Ding, S. Patinet, M. L. Falk, Y. Q. Cheng, and E. Ma, Proc. Natl. Acad. Sci. U. S. A. **111**, 14052 (2014).
[21] R. Milkus and A. Zaccone, Phys. Rev. B **93**, 094204 (2016).
[22] M. Guerdane and H. Teichler, Phys. Rev. Lett. **101**, 065506 (2008).
[23] M. I. Mendelev, M. J. Kramer, R. T. Ott, D. J. Sordelet, D. Yagodin, and P. Popel, Philos. Mag. **89**, 967 (2009).
[24] Y. Zhang, F. Zhang, C. Z. Wang, M. I. Mendelev, M. J. Kramer, and K. M. Ho, Phys. Rev. B **91**, 064105 (2015).
[25] R. E. Ryltsev, B. A. Klumov, N. M. Chtchelkatchev, and K. Y. Shunyaev, J. Chem. Phys. **145**, 034506 (2016).
[26] J. M. Dickey and A. Paskin, Phys. Rev. **188**, 1407 (1969).
[27] J. Bünz, T. Brink, K. Tsuchiya, F. Meng, G. Wilde, and K. Albe, Phys. Rev. Lett. **112**, 135501 (2014).
[28] See Supplementary Material at [insert URL] for details of calculations about sample preparations, structural characterizations and atomic vibrational analyses.
[29] M. Q. Jiang, M. Peterlechner, Y. J. Wang, W. H. Wang, F. Jiang, L. H. Dai, and G. Wilde, Appl. Phys. Lett. **111**, 261901 (2017).
[30] Z. Fan, J. Ding, Q.-J. Li, and E. Ma, Phys. Rev. B **95**, 144211 (2017).
[31] A. Widmer-Cooper, H. Perry, P. Harrowell, and D. R. Reichman, Nat. Phys. **4**, 711 (2008).